ACTA CHEMICA SCANDINAVICA 24 (1970) 1925–1940

Compounds with the Marcasite Type Crystal Structure

V.* The Crystal Structures of FeS_2, $FeTe_2$, and $CoTe_2$

GUNNAR BROSTIGEN and ARNE KJEKSHUS

Kjemisk Institutt A, Universitetet i Oslo, Blindern, Oslo 3, Norway

The crystal structures of the marcasite modifications of FeS_2 (the mineral marcasite), $FeTe_2$, and $CoTe_2$ have been redetermined at room temperature from three-dimensional single crystal X-ray data. Using the Hamilton test in judgements between a number of possible models for each structure the space group was found to be $Pnn2$. Compared with the symmetry hitherto assumed for the FeS_2-m type, these structures lack the mirror plane(s) perpendicular to [001] at $z=\frac{1}{2}$ (and $z=0$). The unit cells contain $2T$ in position (a) with $z=0$ and $4X$ in position (c) with

$x=0.2008(4)$, $y=0.3778(3)$, $z=0.0089(22)$ for FeS_2;
$x=0.2241(1)$, $y=0.3620(1)$, $z=0.0218(28)$ for $FeTe_2$;
$x=0.2204(1)$, $y=0.3636(1)$, $z=0.0007(39)$ for $CoTe_2$.

(Standard deviations are appended in brackets.) Both kinds of atoms show anisotropic thermal motion in the three structures. The possible breakdown of the harmonic approximation for the thermal vibration of S in FeS_2 is discussed briefly. The T atoms are displaced from the centres of the coordination octahedra in FeS_2 and $FeTe_2$, whereas only insignificant off-centre displacements occur in $CoTe_2$ at room temperature. The applicability of the Jahn-Teller theorem in explaining the structural distinctions within the group of compounds with the FeS_2-m and FeS_2-p type structures is discussed and this hypothesis is finally rejected.

The first proposal for the crystal structure of FeS_2-m (m = marcasite) was advanced in 1922 by Huggins [1] on the basis of an assumed analogy with that of FeS_2-p (p = pyrite) [2,3] and inferences from the Lewis [4] theory of atomic structure. The following (1931) structure determination by Buerger [5] ultimately confirmed that Huggins' suggestion was essentially correct, although the crystallographic substantiation of the latter author proved to be incorrect. Subjected to criticism by Pauling and Huggins,[6,7] Buerger [8] repeated the determination in 1937 and confirmed his earlier findings with improved accuracy.

* Part IV. *Acta Chem. Scand.* **23** (1969) 3043.

On the basis of a thorough examination of the systematic extinctions in the diffraction data, Buerger [5] concluded that the structure of FeS_2-*m* belongs to one of the space groups *Pnnm* or *Pnn*2 (using a setting of the unit cell in accordance with Ref. 8). The only essentially unproved assumption in Buergers [5,8] determinations is accordingly his choice of the highest symmetric space group *Pnnm*. This space group has furthermore been uncritically applied in the later structure determinations of the isostructural compounds. A reduction of the symmetry to that of space group *Pnn*2 would, however, provide a virtually identical atomic arrangement for the FeS_2-*m* type structure. This is depicted in Fig. 1 where also the previously mentioned mirror

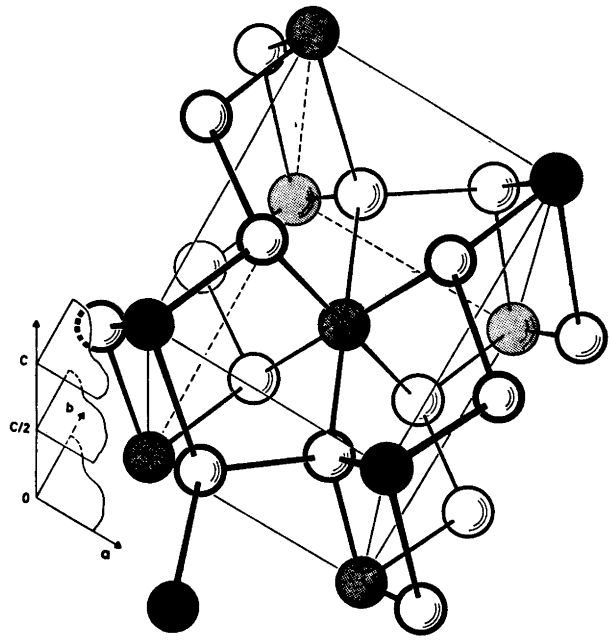

Fig. 1. Model showing the FeS_2-*m* type structure. The shaded circles represent the metal (*T*) atoms and the open circles the non-metal (*X*) atoms. The location of the mirror planes characteristic of space group *Pnnm* is indicated.

planes of symmetry perpendicular to [001] at $z=0$ and $z=\frac{1}{2}$ are indicated. The purpose of the present study was to eliminate the space group ambiguity for the relevant modifications of FeS_2, $FeTe_2$, and $CoTe_2$. (Earlier structure determinations of $FeTe_2$ and $CoTe_2$ are reported by Tengnér [9] and Grønvold *et al.*[10]) A parallel examination of the isostructural compound $FeSb_2$ has also been carried out and although the complete report is published elsewhere [11] a few relevant results are included here for the purpose of comparison.

A verification of the presence or absence of the mirror plane in these structures is, apart from the purely crystallographic merits, of considerable

interest in relation to the applicability of the Jahn-Teller effect as an explanation [12-15] of the occurrence of the two classes [8] of binary compounds with the marcasite type structure.

EXPERIMENTAL

Materials. The pure elements used in this study were 99.99+% Fe and Co (Johnson, Matthey & Co., Ltd.; turnings from rods) and 99.999 % Te (Koch-Light Laboratories, Ltd.).

The high purity *marcasite* (FeS_2) crystals from Joplin, U.S.A. were obtained from Mineralogisk-geologisk museum, Universitetet i Oslo. A mass spectrographic analysis yielded the following impurities (in ppm): F(25), Na(50), Mg(40), Al(100), Si(300), P(5), Cl(<1), K(10), Ca(2), Ti(6), Cr(5), Co(<1), Ni(100), Cu(10), Zn(30), As(10), Se(15), Mo(12), Ag(3), Cd(15), Sb(3), Te(15), and Pb(20). (The contaminations by Al and Si are almost certainly due to feldspar.)

It is worth noting that marcasite crystals from the same source were used by Buerger [5] in this original determination of the structure and that the marcasite from Joplin according to analyses [5,16,17] has a composition corresponding to the stoichiometric formula FeS_2. (A careful visual and X-ray examination of the present sample showed that it also contained small crystals of pyrite.)

Preparations. Single crystals of $FeTe_2$ and $CoTe_2$ were obtained by means of chemical transport reactions using iodine as the transport agent. A temperature gradient of ~1°C/mm was applied along ~200 mm long (evacuated and sealed) silica capsules, while their hot ends, containing stoichiometric mixtures of the elements, were heated at ~500°C. At an iodine concentration of ~0.1 mg/ml capsule volume, a number of $FeTe_2$ crystals were formed in the middle of the capsules after 3 weeks, whereas no visible crystal growth was detected in the capsules containing $CoTe_2$. By increasing the iodine concentration to ~0.4 mg/ml capsule volume a few $CoTe_2$ crystals were produced after 4 months.

Attempts have also been made to synthesize crystals of FeS_2-*m* by this technique. A variety of different thermal conditions and concentrations of the transport agent were tried during these syntheses, but this endeavour failed, the crystals obtained invariably being of the FeS_2-*p* phase.[18]

X-Ray diffraction. X-Ray photographs of crushed crystals were taken in a Guinier focusing camera of 80 mm diameter with monochromatized Cu$K\alpha_1$-radiation ($\lambda = 1.54050$ Å) using KCl ($a = 6.2919$ Å [19]) or Si ($a = 5.4305$ Å [20]) as an internal standard.

Three dimensional single crystal data were collected with an integrating Weissenberg camera of 57.3 mm diameter with Zr-filtered Mo$K\alpha$-radiation using the multiple-film technique. The intensities were measured microphotometrically except for the weakest reflections which were estimated visually by comparison with a standard scale. The intensities were corrected for the combined Lorentz and polarization factors, and for absorption and secondary extinction according to the actual shape of the crystals. (No correction for dispersion was carried out.)

Computations. The computational work, including least squares refinements of the unit cell dimensions, corrections, data reductions, scalings, and full matrix least squares refinements of the structure factors, and calculations of interatomic distances and angles, was performed on the electronic computers UNIVAC 1107 and CDC 3300 using in most cases programmes by Dahl *et al.*[21]

The atomic scattering factors used in the calculations of F_c-values were taken from Hanson *et al.*[22] The extent of the agreement between the observed and calculated structure factor data is judged from the average and weighted reliability factors:

$$R = \sum ||F_o| - |F_c|| / \sum |F_o|$$

$$R^* = [\sum w(|F_o| - |F_c|)^2 / \sum w|F_o|^2]^{\frac{1}{2}}$$

where w denotes the weight factor. The unobserved reflections are not included in the calculations of R and R^*, and are omitted from the least squares refinements. (The observed and calculated structure factor data are available from the authors upon request.)

Throughout this paper the calculated standard deviations are given in parentheses behind the corresponding parameter values. In order to save space only the last digit (or the two last digits) is presented.

RESULTS AND DISCUSSION

(i) *Compositions, unit cell dimensions, and space group.* FeS_2-*m* appears to assume the stoichiometric 1:2 composition without having any appreciable range of homogeneity, whereas the $FeTe_2$ and $CoTe_2$ phases exhibit homogeneity ranges from 66.6 ± 0.2 to 67.4 ± 0.2 and 66.5 ± 0.2 to 69.7 ± 0.2 atomic % Te at 450°C, respectively. The variations of the unit cell dimensions with composition for the latter phases are shown in Fig. 2 a, b together with the

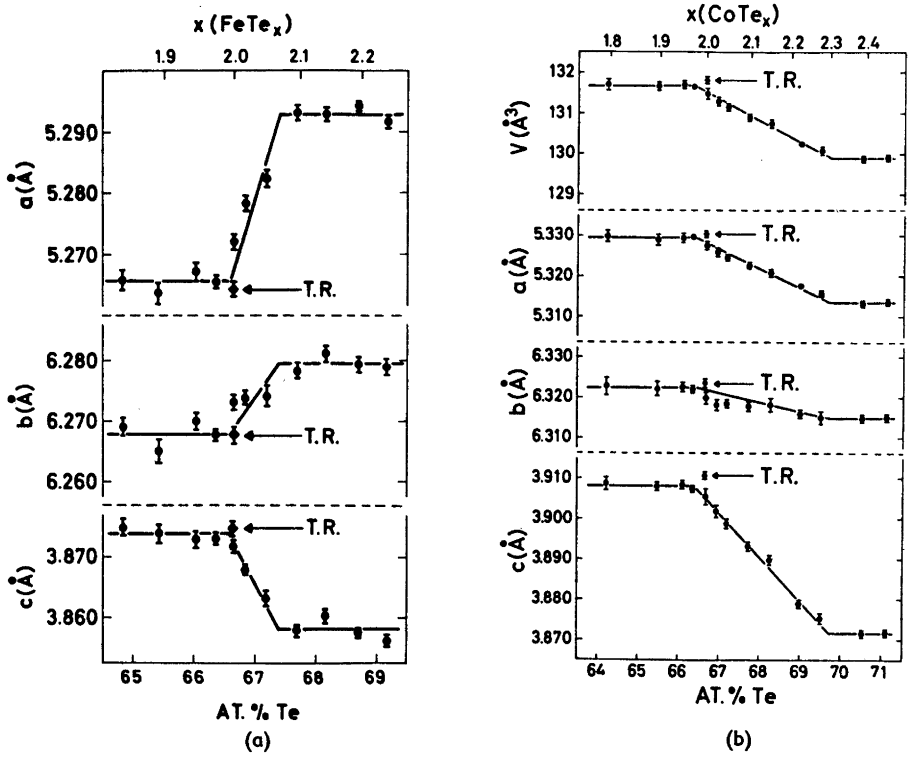

Fig. 2. Unit cell dimensions *versus* composition for the (a) $FeTe_2$ and (b) $CoTe_2$ phases. Results marked ● correspond to powder samples quenched from 450°C and those marked ◆ represent crystals prepared by transport reactions (T.R.). The vertical bars represent the uncertainty when the calculated error limit (twice the standard deviation) exceeds the size of the symbols.

corresponding values for the samples prepared by transport reactions (marked T.R. on the diagrams). These results unequivocally place the compositions of the crystals obtained by the transport reactions at the tellurium-poor end of the homogeneity ranges, thus justifying the use of the stoichiometric formulae $FeTe_2$ and $CoTe_2$. The compositions stated are furthermore supported by the analyses of the structure factor data, since the allowance for variable composi-

tion as a parameter during the refinements invariably lead to atomic ratios X/T within 2.00 ± 0.02 for all three compounds. (An account of the defect structures of the $FeTe_2$ and $CoTe_2$ phases will be presented elsewhere.)

The following unit cell dimensions:

FeS_2:	$a = 4.4431(9)$ Å,	$b = 5.4245(9)$ Å,	$c = 3.3871(6)$ Å
$FeTe_2$:	$a = 5.2655(8)$ Å,	$b = 6.2679(8)$ Å,	$c = 3.8738(7)$ Å
$CoTe_2$:	$a = 5.3294(6)$ Å,	$b = 6.3223(8)$ Å,	$c = 3.9080(6)$ Å

have been obtained for the stoichiometric compositions as average values for several independent samples. According to the observed densities the unit cells contain $2\,TX_2$-groups.

The systematically missing reflections in the diffraction data are of the type $0kl$ absent when $k+l = 2n+1$ and $h0l$ absent when $h+l = 2n+1$ implying that the possible space groups are limited to *Pnnm* and *Pnn2* (*cf.* the introduction).

(ii) *Refinements of the structures.* Least squares refinements were begun at once since the FeS_2-*m* type atomic arrangement assumed earlier is clearly a good approximation to the actual structures of FeS_2, $FeTe_2$, and $CoTe_2$. A determination of possible deviations of the structures from the symmetry of space group *Pnnm* was based on an alternative description of the FeS_2-*m* type structure in terms of *Pnn2*. According to the latter space group the two T atoms occupy position (*a*) $0,0,z$; $\frac{1}{2},\frac{1}{2},\frac{1}{2}+z$ and the four X atoms reside in position (*c*)x,y,z; $\bar{x},\bar{y},z$; $\frac{1}{2}-x, \frac{1}{2}+y, \frac{1}{2}+z$; $\frac{1}{2}+x, \frac{1}{2}-y, \frac{1}{2}+z$. Since only the difference between the z-parameters of T and X is a relevant parameter in this problem, that of the T atoms is equated to zero in the refinements of the positional and thermal parameters.

Seven distinct models (see Table 1), which include the possibility of anisotropic as well as isotropic thermal motion of the atoms, are considered for each of the three structures.* In the cases where anisotropic temperature factors are allowed, it is clear that considerations of symmetry introduce limitations in the values of some of the vibrational parameters β_{ij} in the expression $\exp[-(\beta_{11}h^2+\beta_{22}k^2+\beta_{33}l^2+2\beta_{12}hk+2\beta_{13}hl+2\beta_{23}kl)]$. $\beta_{13}=\beta_{23}=0$ must generally be obeyed for the T atoms, since these lie on twofold axes parallel to [001]. Similarly, the restriction implied by $z=0$ for X places these atoms in mirror planes perpendicular to [001] at $z=0$ and $z=\frac{1}{2}$ (*cf.* Fig. 1), and leads to the identical relation $\beta_{13}=\beta_{23}=0$ appropriate to model No. 2 in Table 1. As seen from Table 1, the same restraints are also placed on the thermal parameters of X in models Nos. 5 and 6 where freedom is allowed to z in order to test the mutual coupling between z on the one hand and β_{13} and β_{23} on the other.

The results listed in Table 1 were obtained by least squares refinements of the structure factor data until no shifts were produced in all variables.

* These models appear to represent the most useful selection, to which may be added a number of special cases, which, however, need not be considered here. It is in principle also possible to construct other more hypothetical models by questioning the correctness of the various symmetry elements of space group *Pnn2*, including the translational symmetry of the lattice. However, such infinitesimal deviations from *Pnn2* are clearly less important and this possibility is therefore neglected in the present investigation.

Table 1. Positional parameters and temperature factors for seven possible refinement models of FeS_2, $FeTe_2$, and $CoTe_2$ according to space group *Pnn*2. (Number of observations, $n=337$, 577, and 665 for FeS_2, $FeTe_2$, and $CoTe_2$, respectively; number of parameters in model No. 7, $m=13$; significance level, $\alpha=0.005$.)

(a) FeS_2

Refined parameters		Restrained models						Unrestrained model
		$z=0$, B_{Fe} and B_S isotropic	$z=0$, $\beta_{13}=\beta_{23}=0$ for S	B_{Fe} and B_S isotropic	B_S isotropic	B_{Fe} isotropic, $\beta_{13}=\beta_{23}=0$ for S	$\beta_{13}=\beta_{23}=0$ for S	
		No. 1	No. 2	No. 3	No. 4	No. 5	No. 6	No. 7
Fe	B	0.15(1)	—	0.15(1)	—	0.15(1)	—	—
	β_{11}	0.0019(1)	0.0024(2)	0.0019(1)	0.0025(2)	0.0019(1)	0.0024(2)	0.0024(2)
	β_{22}	0.0013(1) B	0.0010(2)	0.0013(1) B	0.0010(2)	0.0013(1) B	0.0010(2)	0.0011(2)
	β_{33}	0.0033(2)	0.0020(7)	0.0033(2)	0.0018(7)	0.0033(2)	0.0020(7)	0.0023(7)
	$2\beta_{12}$	—	0.0011(4)	—	0.0012(4)	—	0.0012(4)	0.0010(4)
S	x	0.2007(4)	0.2007(4)	0.2008(4)	0.2008(3)	0.2007(4)	0.2007(4)	0.2008(4)
	y	0.3783(3)	0.3783(3)	0.2783(3)	0.3783(3)	0.3782(3)	0.3782(3)	0.3778(3)
	z	0	0	0.0117(23)	0.0130(22)	0.0135(23)	0.0138(22)	0.0089(22)
	B	0.31(2)	—	0.30(2)	0.29(2)	—	—	—
	β_{11}	0.0039(3)	0.0043(4)	0.0038(3)	0.0037(3)	0.0045(4)	0.0042(4)	0.0042(4)
	β_{22}	0.0026(2) B	0.0023(2)	0.0025(2) B	0.0025(2) B	0.0022(3)	0.0023(3)	0.0026(3)
	β_{33}	0.0068(4)	0.0067(11)	0.0065(4)	0.0063(4)	0.0044(11)	0.0051(12)	0.0067(13)
	$2\beta_{12}$	—	−0.0002(6)	—	—	−0.0001(6)	−0.0003(6)	−0.0004(6)
	$2\beta_{13}$	—	0	—	—	0	0	0.0026(49)
	$2\beta_{23}$	—	0	—	—	0	0	−0.0234(35)
R		0.0652	0.0636	0.0647	0.0628	0.0640	0.0628	0.0618
R^*		0.0964	0.0935	0.0953	0.0923	0.0942	0.0918	0.0895
$\mathscr{R}$		1.077	1.045	1.065	1.031	1.053	1.026	—
$\mathscr{R}_{b,n-m,\alpha}$		1.036	1.020	1.033	1.025	1.025	1.016	—
b		9	3	8	5	5	2	—

(b) $FeTe_2$

Refined parameters		Restrained models						Unrestrained model
		$z=0$, B_{Fe} and B_{Te} isotropic	$z=0$, $\beta_{13}=\beta_{23}=0$ for Te	B_{Fe} and B_{Te} isotropic	B_{Te} isotropic	B_{Fe} isotropic, $\beta_{13}=\beta_{23}=0$ for Te	$\beta_{13}=\beta_{23}=0$ for Te	
		No. 1	No. 2	No. 3	No. 4	No. 5	No. 6	No. 7
Fe	B	0.23(2)	—	0.19(2)	—	0.19(2)	—	—
	β_{11}	0.0021(2)	0.0026(3)	0.0017(2)	0.0023(3)	0.0017(2)	0.0023(3)	0.0025(3)
	β_{22}	0.0015(1) B	0.0011(2)	0.0012(1) B	0.0011(2)	0.0012(1) B	0.0011(2)	0.0012(2)
	β_{33}	0.0038(3)	0.0045(34)	0.0032(3)	−0.0043(35)	0.0032(3)	−0.0040(35)	0.0006(36)
	$2\beta_{12}$	—	−0.0005(5)	—	−0.0005(4)	—	−0.0007(4)	−0.0008(5)
Te	x	0.2241(1)	0.2241(1)	0.2241(1)	0.2240(1)	0.2241(1)	0.2241(1)	0.2241(1)
	y	0.3620(1)	0.3620(1)	0.3620(1)	0.3620(1)	0.3620(1)	0.3620(1)	0.3620(1)
	z	0	0	0.0273(23)	0.0279(22)	0.0279(23)	0.0285(22)	0.0218(28)
	B	0.36(1)	—	0.36(1)	0.36(1)	—	—	—
	β_{11}	0.0032(1)	0.0031(3)	0.0032(1)	0.0032(1)	0.0031(1)	0.0031(3)	0.0032(1)
	β_{22}	0.0023(1) B	0.0023(2)	0.0023(1) B	0.0023(1) B	0.0023(1)	0.0023(1)	0.0023(1)
	β_{33}	0.0060(2)	0.0055(15)	0.0060(2)	0.0060(2)	0.0077(15)	0.0074(15)	0.0087(15)
	$2\beta_{12}$	—	−0.0004(2)	—	—	−0.0005(2)	−0.0005(2)	−0.0005(2)
	$2\beta_{13}$	—	0	—	—	0	0	0.0061(11)
	$2\beta_{23}$	—	0	—	—	0	0	−0.0047(9)
R		0.0782	0.0776	0.0760	0.0756	0.0747	0.0743	0.0737
R^*		0.1202	0.1189	0.1144	0.1135	0.1132	0.1123	0.1112
$\mathscr{R}$		1.081	1.069	1.029	1.021	1.018	1.009_9	—
$\mathscr{R}_{b,n-m,\alpha}$		1.021	1.012	1.020	1.015	1.015	1.009_6	—
b		9	3	8	5	5	2	—

(c) $CoTe_2$

Refined parameters		Restrained models						Unrestrained model
		$z=0$, B_{Co} and B_{Te} isotropic	$z=0$, $\beta_{13}=\beta_{23}=0$ for Te	B_{Co} and B_{Te} isotropic	B_{Te} isotropic	B_{Co} isotropic, $\beta_{13}=\beta_{23}=0$ for Te	$\beta_{13}=\beta_{23}=0$ for Te	
		No. 1	No. 2	No. 3	No. 4	No. 5	No. 6	No. 7
Co	B	0.40(2)	—	0.37(3)	—	0.37(3)	—	—
	β_{11}	0.0035(2)	0.0044(4)	0.0033(3)	0.0042(4)	0.0033(3)	0.0042(4)	0.0045(4)
	β_{22}	0.0025(1) B	0.0023(3)	0.0023(3) B	0.0022(3)	0.0023(3) B	0.0022(3)	0.0024(3)
	β_{33}	0.0065(3)	0.0042(22)	0.0061(5)	−0.0002(25)	0.0061(5)	0.0001(24)	0.0058(23)
	$2\beta_{12}$	—	0.0003(6)	—	0.0004(6)	—	0.0003(6)	0.0003(6)
Te	x	0.2204(1)	0.2204(1)	0.2204(1)	0.2204(1)	0.2204(1)	0.2204(1)	0.2204(1)
	y	0.3636(1)	0.3636(1)	0.3636(1)	0.3636(1)	0.3636(1)	0.3636(1)	0.3636(1)
	z	0	0	0.0156(30)	0.0181(27)	0.0175(28)	0.0198(25)	0.0007(39)
	B	0.38(1)	—	0.38(1)	0.38(1)	—	—	—
	β_{11}	0.0033(1)	0.0034(1)	0.0033(1)	0.0033(1)	0.0034(1)	0.0034(1)	0.0036(1)
	β_{22}	0.0024(1) B	0.0023(1)	0.0024(1) B	0.0024(1) B	0.0023(1)	0.0023(1)	0.0024(1)
	β_{33}	0.0062(2)	0.0079(8)	0.0062(2)	0.0062(2)	0.0086(8)	0.0085(8)	0.0103(10)
	$2\beta_{12}$	—	−0.0009(2)	—	—	−0.0009(2)	−0.0009(2)	−0.0009(2)
	$2\beta_{13}$	—	0	—	—	0	0	0.0063(9)
	$2\beta_{23}$	—	0	—	—	0	0	0.0052(9)
R		0.0896	0.0874	0.0893	0.0886	0.0867	0.0860	0.0846
R *		0.1161	0.1134	0.01155	0.1146	0.1129	0.1121	0.1110
$\mathscr{R}$		1.046	1.022	1.041	1.032	1.017	1.010	—
$\mathscr{R}_{b,n-m,\alpha}$		1.018	1.010	1.017	1.013	1.013	1.008	—
b		9	3	8	5	5	2	—

Careful attention was paid to the scaling problem in order to avoid this factor enforcing preference of a particular model. Different sets of input parameters were furthermore tried for each model in order to ascertain that none of the least square refinements was terminated at secondary (false) minima. This is in accordance with expectations, in view of the rather favourable ratios between the numbers of observations and variables (26, 44, and 51 for the unrestrained models of FeS_2, $FeTe_2$, and $CoTe_2$, respectively). The coefficients for correlation between the various variables were found to have satisfactory values in all cases.

According to the significance test of Hamilton,[23] the probable correctness of the various models is judged by comparison of $\mathscr{R}$ $(=R_r^*/R_u^*$, where R_r^* and R_u^* correspond to the weighted reliability factors for restrained and unrestrained models, respectively) with $\mathscr{R}_{b,n-m,\alpha}$ (where b is the dimension of the assumed hypothesis, $n-m$ the degrees of freedom of the data, and α the significance level). Application of this test on the data in Table 1 leads to rejection of models Nos. $1-6$ at significance levels <0.005 for the three compounds. The unrestrained model No. 7 is accordingly favoured by the Hamilton test in all cases and this fact is furthermore supported by comparison of the values of the variable parameters with their associated standard deviations (Table 1). Although this conclusion is common to the three structures, there are also noteworthy individual variations.

In the case of FeS_2 the mirror plane perpendicular to [001] is missing due to the fact that z_S departs significantly from zero, whereas the thermal parameters do not contribute any specific information about this question. Both kinds of atoms exhibit anisotropic thermal motion. The conventional vibration ellipsoid model may be applied to the Fe atoms, whereas this model fails to describe the thermal motion of the S atoms because of the negative value obtained for $(\beta_{22}\beta_{33}-\beta_{23}^2)$ in this case. Neglecting the possibility that the failure is caused by systematic errors in the structure factor data, it may be suggested that this result demonstrates the inadequacy of the harmonic approximation in describing the thermal vibrations in FeS_2. Anharmonic effects are clearly present in any real crystal, as, for example, evidenced by the occurrence of thermal expansion which otherwise would be lacking. However, it has only rather recently been recognized (*cf.* Willis [24]) that the effect of anharmonicity must be considered in order to account completely for the reduction in intensity of the Bragg reflections caused by the thermal motions of the atoms. The experimental and theoretical approaches of this problem by Willis [24] have been confined to isotropic cases, whereas no attempt appears to have been made to attack the general problem with anharmonicity in admixture with anisotropic thermal vibration. A more detailed analysis of the FeS_2 structure according to such an improved model was considered to be outside the scope of the present study, but the problem merits attention and will be investigated further.

The structure of $FeTe_2$ departs significantly from the symmetry of space group *Pnnm* both with respect to positional and thermal parameters (*cf.* Table 1b). The final value $z_{Te}=0.0218$ differs from 0 by approximately 8 standard deviations. Anisotropic thermal vibration is found for both kinds

of atoms and their motions may be described by the ellipsoid model, which implies that the harmonic approximation apparently is satisfied in this case.

During the refinement of the $CoTe_2$ structure from model No. 6 to No. 7 the value of z_{Te} converged very slowly (more than 20 iterations by the method of least squares were required) to approximately zero, while β_{13} and β_{23} for Te (and β_{33} for Co!) similarly assumed values significantly different from zero. The systematic shifts in the parameters demonstrated the necessity of continuing the refinement process even when the shifts became less than the corresponding standard deviation.

The fact that z_{Te} obtains a value which is only insignificantly different from zero in the preferred model No. 7 (Table 1c) does not imply that the mirror planes perpendicular to [001] at $z=0$ and $z=\frac{1}{2}$ are present in the structure of $CoTe_2$. By reason of symmetry the presence of the mirror planes would require both $z=0$ and $\beta_{13}=\beta_{23}=0$ for the Te atoms (*vide supra*). The latter requirements correspond to the restraints imposed by model No. 2 which, however, is to be rejected in favour of model No. 6 as well as No. 7 at a significance level <0.005. The conclusion is therefore that the mirror plane definitely is lacking in the structure of $CoTe_2$. Both kinds of atoms are found to vibrate anisotropically and the harmonic approximation of the ellipsoid model appears to be appropriate.

The orientation and amplitudes (magnified 10 times relative to the dimensions of the unit cell) of the thermal vibration ellipsoids, as derived from the parameters in Table 1, are illustrated in Fig. 3, which also includes the corresponding data for $FeSb_2$.[11] The thermal motion of S in the structure of FeS_2 is shown as a cross, the size of which indicates the magnitude of its oscillation as the average of the amplitudes corresponding to β_{11}, β_{22}, and β_{33} in Table 1a, model No. 7. The orientations of the ellipsoids are plausible from a steric point of view, since these coincide with favourable directions in the crystal lattices where the free (unoccupied) space is at a maximum. The directions of the maximum amplitudes of atomic oscillations may be explained in this way, whereas it is inherently more difficult to account for the individual variations in orientation, shape, and size of the different ellipsoids depicted in Fig. 3.

The present values for the positional parameters x and y (see model No. 7, Table 1 a–c) are in good agreement with those reported earlier.[5,8–10] In view of the controversy between Pauling and Huggins [6,7] on the one hand and Buerger [5,8] on the other, it is of particular interest to note that the best x,y parameters found by Buerger [8] accord within two standard deviations with those listed in Table 1.

(iii) *Discussion of the structures.* Important interatomic distances and angles calculated from the unit cell dimensions and the positional parameters for model No. 7 in Table 1 a–c are given in Table 2, including also the data for $FeSb_2$ for the purpose of comparison. The lengths of the shortest interatomic distances in the table definitely confirm that these represent bonding distances, the values showing good conformity with the corresponding expected values for single $T-X(,X-T,)$ and $X-X$ bonds. Each T atom in the structures is therefore considered as covalently bonded to the six, octahedrally coordinated X atoms by shared (single) electron pairs and each X atom is similarly bonded

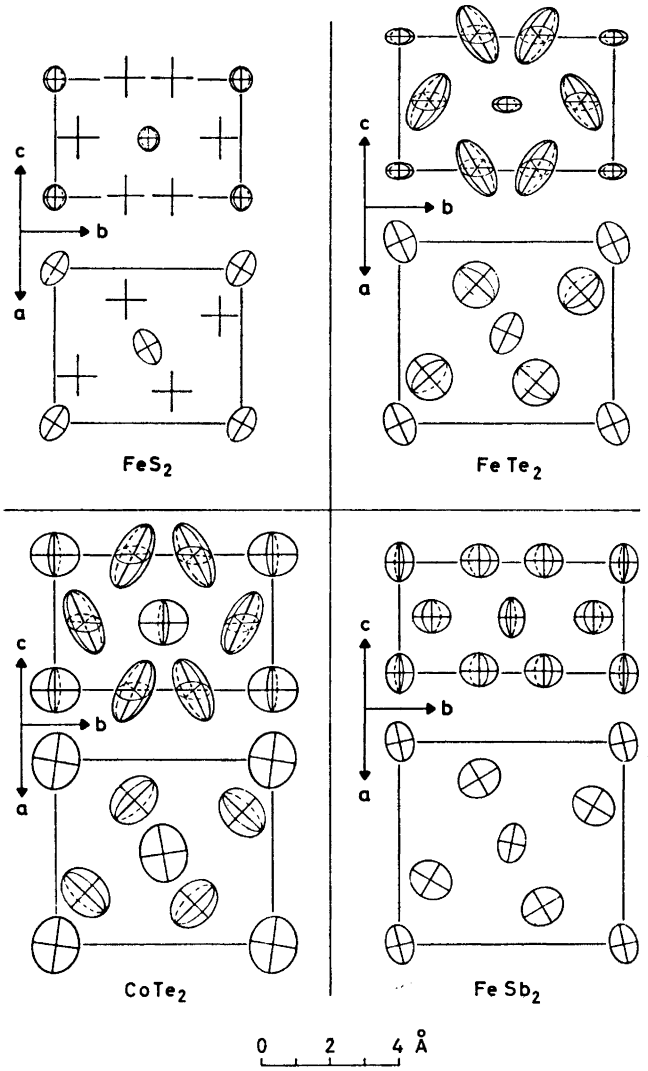

Fig. 3. Ellipsoids of thermal motion in the structures of FeS_2, $FeTe_2$, $CoTe_2$, and $FeSb_2$ viewed along [001] and [100]. The centres of the ellipsoids correspond to the positions of the atoms. Sections through pairs of the principle axes are projected, thus forming the three ellipses (the degenerate form is a line) shown in each case. Scale $\times 10$ for the vibration amplitudes. (The shape and orientation of the ellipsoids have uncertainties which are not evident from the diagrams; *cf.* Table 1a–c.)

to three T and one X in a tetrahedral arrangement (*cf.* Fig. 1). The shortest $T-T$ and next shortest $T-X$ (beyond the bonding) and $X-X$ distances may be interpreted as caused by the geometry of the crystal structures and these and longer distances are accordingly characterized as essentially non-

Table 2. Some important interatomic distances and angles (with standard deviations) in the crystal structures of FeS_2, $FeTe_2$, $CoTe_2$, and $FeSb_2$. The data are calculated from the unit cell dimensions and the positional parameters for model No. 7 in Table 1, except those for $FeSb_2$, which are quoted from Holseth and Kjekshus.[11]

Interatomic distances (Å)					Interatomic angles (°)				
Compound	FeS_2	$FeTe_2$	$CoTe_2$	$FeSb_2$	Compound	FeS_2	$FeTe_2$	$CoTe_2$	$FeSb_2$
$T-X(2)$ [a]	2.230(6)	2.508(8)	2.602(11)	2.5782(11)	$X-T-X(1)$	81.5(2)	79.8(2)	82.7(3)	102.95(4)
$T-X(2)$ [a]	2.235(2)	2.5589(7)	2.5815(6)	2.5762(6)	$X-T-X(1)$	83.5(2)	84.8(2)	82.8(3)	105.11(4)
$T-X(2)$ [a]	2.275(6)	2.635(8)	2.606(11)	2.6164(11)	$X-T-X(2)$	87.5(2)	86.4(2)	88.0(3)	87.95(3)
					$X-T-X(2)$	88.6(2)	89.2(2)	88.1(3)	88.78(3)
					$X-T-X(2)$	91.4(2)	90.7(2)	91.9(3)	91.19(3)
					$X-T-X(2)$	92.6(2)	93.6(2)	92.0(3)	92.06(3)
					$X-T-X(2)$	97.5(2)	97.7(2)	97.2(3)	75.97(4)
$X-T(1)$ [a]	2.230(6)	2.508(8)	2.602(11)	2.5782(11)	$T-X-T(1)$	97.5(2)	97.7(2)	97.2(3)	75.97(4)
$X-T(1)$ [a]	2.235(2)	2.5589(7)	2.5815(6)	2.5762(6)	$T-X-T(1)$	119.3(3)	121.3(3)	123.6(5)	127.81(5)
$X-T(1)$ [a]	2.275(6)	2.635(8)	2.606(11)	2.6164(11)	$T-X-T(1)$	121.4(3)	126.7(3)	123.8(5)	129.57(5)
$X-X(1)$ [a]	2.223(3)	2.9261(11)	2.9143(11)	2.8871(12)	$X-X-T(1)$	103.09(8)	98.76(2)	99.22(2)	105.32(2)
					$X-X-T(1)$	107.2(3)	104.5(3)	105.4(4)	107.18(4)
					$X-X-T(1)$	107.5(3)	105.3(3)	105.4(4)	107.45(4)
$T-X$ [b]	3.491(2)	4.1702(7)	4.1915(6)	4.0818(13)					
$X-X$ [b]	2.971(3)	3.382(2)	3.4433(11)	3.1973(3)					
$T-T$ [b]	3.3871(6)	3.8738(7)	3.9080(6)	3.1973(3)					

[a] Bonding interatomic distances. [b] Shortest interatomic distances neglected as bonding.

bonding in Table 2. A more detailed discussion of the chemical bonding in the compounds with the FeS_2-*m* type structure will be presented in a forthcoming paper.[25]

Due to the lacking mirror plane in space group *Pnn*2 there occur three non-equivalent bonding $T-X$ distances (*cf.* Table 2). In the structures of FeS_2 and $FeSb_2$ one of these $T-X$ distances (notably one of the two which would have been identical in *Pnnm*) differ highly significantly from the others according to the significance test of Cruickshank.[26,27] The mutual differences between the three distances are all highly significant in the structure of $FeTe_2$, whereas the corresponding differences in the case of $CoTe_2$ must be placed in the possibly significant and not significant categories.

Compared with the current conceptions on the atomic arrangement in the FeS_2-*m* type structure the revised data imply a small, but not insignificant, increase in the irregularity of the coordination polyhedra around the T and X atoms. The most conspicuous difference concerns the shifting of the T atoms from the centres of the surrounding X_6 octahedra. These displacements take place along [001], where the X_6 octahedra mutually share edges (*cf.* Fig. 1), and their magnitudes (which amount to $z_X \cdot c$) are listed in Table 3. The displace-

Table 3. Displacement of T and $X-X$ edge lengths of octahedra (in Å) in the crystal structures of FeS_2, $FeTe_2$, $CoTe_2$, and $FeSb_2$ (at room temperature).

Compound		FeS_2	$FeTe_2$	$CoTe_2$	$FeSb_2$
Magnitude of T displacement [a]		0.030(7)	0.084(11)	0.003(15)	0.031(2)
"Fully relaxed" edge lengths	$X-X(2)$ [a]	3.3871(6)	3.8738(7)	3.9080(6)	3.1973(3)
	$X-X(2)$ [b]	2.971(2)	3.382(1)	3.443(1)	4.094(1)
	Average	3.179	3.628	3.676	3.646
"Relatively unrelaxed" edge lengths	$X-X(4)$	3.119(6)	3.557(8)	3.603(11)	3.606(1)
	$X-X(4)$	3.227(6)	3.694(8)	3.730(11)	3.710(1)
	Average	3.173	3.626	3.666	3.658

[a] Parallel to [001]. [b] Perpendicular to [001]; edge shared with adjacent octahedra above or below.

ments are obviously significant in all cases, except for that of $CoTe_2$. It is relevant to emphasize that the present results refer to the situation at room temperature, since the magnitude of the displacement almost certainly must be temperature dependent due to its association with the thermal vibrations in the lattice. On general grounds, it is expected that the effect should be most pronounced at low temperatures where the amplitudes of thermal vibration as well as their inherent anisotropy will finally become negligible. In the case of $CoTe_2$, where a marked coupling between the thermal parameters β_{33} for Co and β_{13} and β_{23} for Te on the one hand and z_{Te} on the other is evident at room temperature (*cf.* Table 1c) the displacement of the Co atoms ought consequently become significant at lower temperatures.

A simple explanation of the off-centre displacement of "cations" in octahedral environment has recently been published by Megaw,[28] who points out (see also Orgel [29]) that the effect depends on the effective radius (not any of the conventional schemes of radii) of T relative to that of X. The off-centre displacement occurs, according to Megaw, when the (hypothetical) unstressed $T-X$ bond length is less than $1/\sqrt{2}$ times the effective diameter of X (which is assumed to correspond to the $X-X$ distance along the edges of the octahedron in the concrete cases considered by her). For a symmetrically placed T atom, this condition gives rise to tension in the diametral $X-T-X$ links within the octahedron, which in turn causes compression in the $X-X$ edges. The elementary Born-theory treatment by Megaw shows that for an isolated octahedron the tension will be relaxed by an off-centre displacement of T, thus sharing the relaxation with the $X-X$ edges which are elongated. (All interatomic forces are assumed to be central.)

In the present structures the T atom is displaced towards the midpoint of the $X-X$ edge parallel to (001) and the displacement is accordingly of the two-corner type within the TX_4 octahedron plane perpendicular to (001). According to the qualitative considerations of Megaw,[28] the four $X-X$ edges in this octahedron plane are expected to be fully relaxed, while the eight $X-X$ edges inclined to it should be relatively unrelaxed. The data in Table 3 are not inconsistent with these expectations, but the large scatter within the two categories of octahedron edge lengths makes it impossible to draw a definite conclusion. However, the concept of an isolated octahedron is clearly a rather crude approximation in the case of the FeS_2-m type structure, where the principal source for the distortion of the octahedron (as well as of the tetrahedron) must be sought among those factors (*cf.* Ref. 25) which determine the overall geometry of the atomic arrangement (Fig. 1). The only testable effect according to Megaws model (*vide supra*) represents, therefore, merely a small superposition on the larger distortion caused by the more important bonding factors, which for one thing are responsible for the distinctly different character of the deformations of the coordination polyhedra in the structure of $FeSb_2$ in comparison with the three others.

The data available at present shed light on the applicability of the Jahn-Teller theorem in explaining the distinction between the two classes

(A) $Mo_{2/3}As_2$, $CrSb_2$, FeP_2, $FeAs_2$, $FeSb_2$, RuP_2, $RuAs_2$, $RuSb_2$, OsP_2, $OsAs_2$, and $OsSb_2$; specified by $c/a \approx 0.55$, $c/b \approx 0.48$

and

(B) FeS_2, $FeSe_2$, $FeTe_2$, "$OsTe_2$", $NiAs_2$, $NiSb_2$, $CoSe_2$, $CoTe_2$, and $CuSe_2$; specified by $c/a \approx 0.74$, $c/b \approx 0.62$

of binary transition metal compounds with the FeS_2-m type structure and their relation to those

MnS_2, $MnSe_2$, $MnTe_2$, FeS_2, $FeSe_2$, $FeTe_2$, RuS_2, $RuSe_2$, $RuTe_2$, OsS_2, $OsSe_2$, $OsTe_2$, "$Rh_{2/3}S_2$", "$Rh_{2/3}Se_2$", "$Rh_{2/3}Te_2$", "$Ir_{2/3}S_2$", "$Ir_{2/3}Se_2$", "$Ir_{2/3}Te$", NiP_2, $NiAs_2$, $NiSb_2$, $PdAs_2$, $PdSb_2$, PtP_2, $PtAs_2$, $PtSb_2$, $PtBi_2$, CoS_2, $CoSe_2$, $CoTe_2$, $AuSb_2$, NiS_2, $NiSe_2$, $NiTe_2$, CuS_2, $CuSe_2$, $CuTe_2$, ZnS_2, $ZnSe_2$, CdS_2, and $CdSe_2$

with the FeS_2-p type structure. The compounds with Jahn-Teller unstable configurations of localized d-electrons on T should, according to Hulliger and Mooser,[12,13] belong to class A (which they therefore name Jahn-Teller marcasites), while those with the ditto stable configurations should crystallize in the FeS_2-p type structure. Hulliger and Mooser justify this basis of their model by stating that the TX_6 octahedron is more deformed in the structures appurtenant to class A than in those of class B and the FeS_2-p type.

The following facts contradict the use of the Jahn-Teller effect as an explanation of the particularities within the marcasite family:

(1) The effect offers no explanation to the existence of class B for the binary compounds as well as the accompanied transitional class A/B of ternary phases with axial proportions intermediate between those of the classes A and B. (Hulliger and Mooser [12,13] are well aware of this failure which accordingly lead them to designate class B as anomalous marcasites.)

(2) Hulliger and Mooser base the considerations on the deviations of the octahedral angles from the ideal value of 90°. The new and more precise structural data for FeS_2-*p*, FeS_2-*m*, $FeTe_2$-*m*, $CoTe_2$-*m*, and $FeSb_2$ show that the average deviations (numerical) in the octahedral angles from 90° are 4.4, 3.8, 4.0, 3.7, and 5.8°, respectively. (Taking the root-mean-square deviations, as Hulliger and Mooser apparently do, leads to the slightly different values 4.4, 4.7, 5.0, 4.5, and 8.2°, respectively.) These figures do therefore not bring out any marked differences between $FeSb_2$ of class A on the one hand and FeS_2-*p* and the representatives FeS_2-*m*, $FeTe_2$-*m*, and $CoTe_2$-*m* of class B on the other.

Bond angles are commonly regarded as considerably less sensitive parameters in the energetic sense than bond lengths. Hence, the relative energies of the electronic bands and/or levels are expectedly not appreciably affected by differences of several degrees in the bond angles (*viz.* smaller deviations from ideal bond angles). Little significance may accordingly be attached to band structure considerations based on bond angles only.

Completely regular symmetry of both kinds of coordination polyhedra is, furthermore, unattainable within the frame of the FeS_2-*m* and FeS_2-*p* type structures (*i.e.* retaining the composition TX_2, the octahedral and tetrahedral configurations of near neighbours around T and X, respectively, and the characteristic $X-X$ pairs).[25] It is, therefore, meaningless to discuss the cause of the deformation of the octahedron without considering the contemporary irregularity of the tetrahedron.

(3) Off-centre displacements of the T atoms are demonstrated for compounds of both class A ($FeSb_2$) and B (FeS_2 and $FeTe_2$), whereas only infinitesimal displacements may occur in the FeS_2-*p* structure.[18] The fact that there is no distinction between the classes A and B in this respect implies that the displacements cannot be a consequence of the Jahn-Teller effect. These findings suggest furthermore that the Jahn-Teller effect is not operative in the structures belonging to class A, since the off-centre displacement alone is sufficient to completely remove the degeneracy of the *d*-levels.

(4) The structure of $Mo_{2/3}As_2$[30] shows all the characteristic features of class A and does therefore definitely belong to this class. Very probable valences for the components lead to a d^0 configuration (*i.e.* no localized 4*d* electrons) on the Mo atoms (*cf.* Ref. 25). The Jahn-Teller effect must thus clearly be rejected as a general explanation of the existence of class A.

(5) Two of the modifications of sodium hyperoxide crystallize with the FeS_2-*m* and FeS_2-*p* type structures.[31] It would be absolutely unreasonable to assume that electrons in *d* orbitals on the Na^+ ions govern the occurrence and relative stability of these structure types for NaO_2.

On the basis of the points 1 – 5 it can be safely concluded that the Jahn-Teller effect must be rejected as an explanation of the structural distinctions

within the group of compounds with the FeS_2-*m* and FeS_2-*p* type structures. Although this basis of Hulliger and Moosers [12,13] model is erroneous, other parts of it appear to need only minor adjustments (*cf.* Ref. 25).

REFERENCES

1. Huggins, M. L. *Phys. Rev.* **19** (1922) 369.
2. Bragg, L. W. *Proc. Roy. Soc. (London)* **A 89** (1914) 468.
3. Ewald, P. P. and Friedrich, W. *Ann. Phys.* **44** (1914) 1183.
4. Lewis, G. N. *J. Am. Chem. Soc.* **38** (1916) 762.
5. Buerger, M. J. *Am. Mineralogist* **16** (1931) 361.
6. Pauling, L. and Huggins, M. L. *Z. Krist.* **87** (1934) 222.
7. Huggins, M. L. *Z. Krist.* **96** (1937) 384.
8. Buerger, M. J. *Z. Krist.* **97** (1937) 504.
9. Tengnér, S. *Z. anorg. allgem. Chem.* **239** (1938) 126.
10. Grønvold, F., Haraldsen, H. and Vihovde, J. *Acta Chem. Scand.* **8** (1954) 1927.
11. Holseth, H. and Kjekshus, A. *Acta Chem. Scand.* **23** (1969) 3043.
12. Hulliger, F. and Mooser, E. *Progr. Solid State Chem.* **2** (1965) 330.
13. Hulliger, F. and Mooser, E. *J. Phys. Chem. Solids* **26** (1965) 429.
14. Pearson, W. B. *Z. Krist.* **121** (1965) 449.
15. Hulliger, F. *Structure and Bonding* **4** (1968) 83.
16. Allen, E. T., Crenshaw, J. L., Johnston, J. and Larsen, E. S. *Z. anorg. Chem.* **76** (1912) 254.
17. Buerger, M. J. *Am. Mineralogist* **19** (1934) 37.
18. Brostigen, G. and Kjekshus, A. *Acta Chem. Scand.* **23** (1969) 2186.
19. Hambling, P. G. *Acta Cryst.* **6** (1953) 98.
20. Parrish, W. *Acta Cryst.* **13** (1960) 838.
21. Dahl, T., Gram, F., Groth, P., Klewe, B. and Rømming, C. *To be published.*
22. Hanson, H. P., Herman, F., Lea, J. D. and Skillman, S. *Acta Cryst.* **17** (1964) 1040.
23. Hamilton, W. C. *Acta Cryst.* **18** (1965) 502.
24. Willis, B. T. *Acta Cryst.* **A 25** (1969) 277.
25. Brostigen, G. and Kjekshus, A. *Acta Chem. Scand. In press.*
26. Cruickshank, D. W. J. *Acta Cryst.* **2** (1949) 65.
27. Cruickshank, D. W. J. and Robertson, A. P. *Acta Cryst.* **6** (1953) 698.
28. Megaw, H. D. *Acta Cryst.* **B 24** (1968) 149.
29. Orgel, L. E. *Discussions Faraday Soc.* **26** (1958) 138.
30. Brown, A. *Nature* **206** (1965) 502; *Private communication.*
31. Carter, G. F. and Templeton, D. H. *J. Am. Chem. Soc.* **75** (1953) 5247.

Received October 16, 1969.